microPublication BIOLOGY

2/14/2023 - *Open Access*

Germline TFAM levels regulate mitochondrial DNA copy number and mutant heteroplasmy in *C. elegans*

Aaron Z.A. Schwartz[1,2], Jeremy Nance[1,2§]

[1]Department of Cell Biology, NYU Grossman School of Medicine, New York NY 10016

[2]Skirball Institute of Biomolecular Medicine, NYU Grossman School of Medicine, New York NY 10016

[§]To whom correspondence should be addressed: jeremy.nance@nyulangone.org

Abstract

The mitochondrial genome (mtDNA) is packaged into discrete protein-DNA complexes called nucleoids. mtDNA packaging factor TFAM (mitochondrial transcription factor-A) promotes nucleoid compaction and is required for mtDNA replication. Here, we investigate how changing TFAM levels affects mtDNA in the *Caenorhabditis elegans* germ line. We show that increasing germline TFAM activity boosts mtDNA number and significantly increases the relative proportion of a selfish mtDNA mutant, *uaDf5*. We conclude that TFAM levels must be tightly controlled to ensure appropriate mtDNA composition in the germ line.

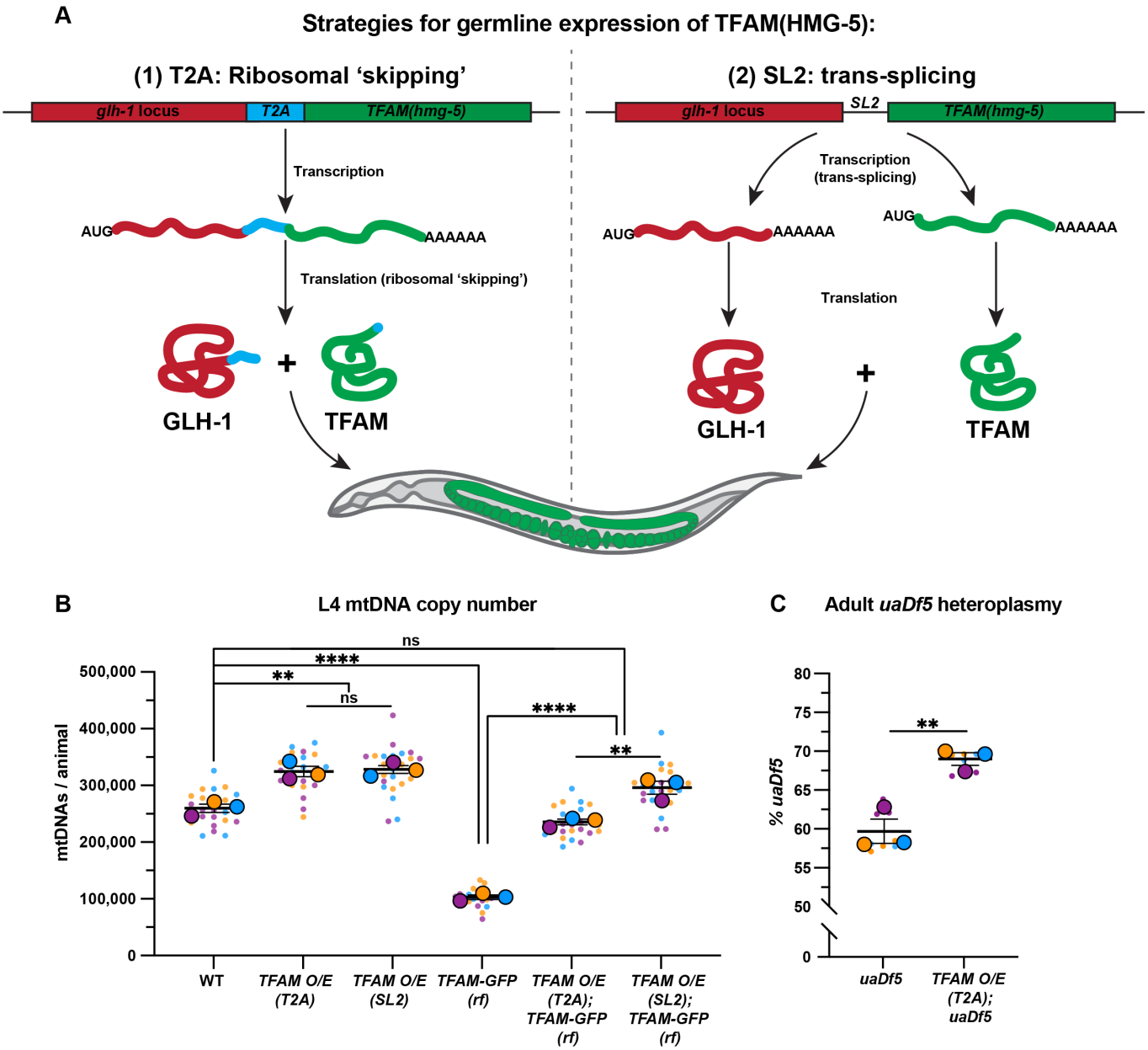

Figure 1. Putative germline TFAM overexpression modulates mtDNA copy number and heteroplasmy:

(**A**) Schematic of strategies to increase germline TFAM levels via transgenic expression at the endogenous *glh-1* locus. Strategy (1) utilizes the viral T2A ribosomal skipping sequence: sequence encoding *T2A::TFAM* was inserted in frame with the endogenous *glh-1* coding sequence, resulting in the production of a single mRNA that is translated into two independent polypeptides via ribosomal skipping of the T2A sequence. Strategy (2) utilizes the *C. elegans SL2* trans-splicing recognition sequence of the gene *rla-1*: sequence encoding *SL2::TFAM* was inserted immediately following the endogenous *glh-1* stop codon, resulting in the production of two independent mRNAs that could then be translated into two polypeptides independently of each other. Endogenous *glh-1* sequence (maroon), *TFAM(hmg-5)* sequence (green), *T2A* sequence (cyan), *SL2* trans-splicing recognition sequence [black line between *glh-1* and *TFAM(hmg-5)*]. (**B**) Quantification of total mtDNA copy number from whole L4 larvae by qPCR in wild-type, *TFAM-O/E (T2A)*, *TFAM-O/E (SL2)*, *TFAM-GFP (rf)*, *TFAM-O/E (T2A); TFAM-GFP (rf)*, and *TFAM-O/E (SL2); TFAM-GFP (rf)* animals. (**C**) Quantification of *uaDf5* heteroplasmy in *uaDf5* and *TFAM-O/E (T2A); uaDf5* adults. Small dots are data points from individual L4 worms in (B), and technical ddPCR replicates in (C), from each of three color-coded biological replicates; the mean from each replicate is shown as a larger circle, the mean of means as a horizonal line, and the S.E.M as error bars. n.s., not significant ($p > 0.05$), ** $p \leq 0.01$, **** $p \leq 0.0001$, unpaired two-tailed Student's *t*-test.

Description

The mitochondrial transcription factor-A (TFAM) plays essential roles in regulating mtDNA copy number, compacting nucleoids, and replicating/transcribing mtDNA (Garrido et al. 2003, Lewis et al. 2016, Fu et al. 2020). Global reduction of TFAM activity has a conserved effect on mtDNA copy number in metazoans: genetic knockdown severely reduces mtDNA levels in mammals, fish, flies, and cell culture systems (Larsson et al. 1998, Kanki et al. 2004, Matsushima et al. 2004, Otten et al. 2020, Wang et al. 2021). The effects of TFAM overexpression on mtDNA levels are less clear. Various studies in cell culture demonstrate that TFAM overexpression can be both sufficient (Kanki et al. 2004, Matsushima et al. 2004), and insufficient (Maniura-Weber et al. 2004) to drive increases in mtDNA. The situation *in vivo* is similar, as two independent studies in *Drosophila* saw no net effect of TFAM overexpression on mtDNA levels (Matsuda et al. 2013, Cagin et al. 2015), whereas TFAM overexpression in mice was sufficient to drive mtDNA expansion above normal levels (Ekstrand et al. 2004). Previously, we and others showed that global reduction in TFAM activity has a profound negative impact on mtDNA levels in *C. elegans*, as expected (Sumitani et al. 2011, Lin et al. 2016, Schwartz et al. 2022). Here we ask the converse: is germline overexpression of the worm *TFAM* homolog, *hmg-5*, sufficient to increase mtDNA levels *in vivo*?

To overexpress TFAM (encoded by the *hmg-5* gene) in the germ line, we used regulatory elements from the endogenous *glh-1* gene, which encodes a highly expressed germline-specific protein (Marnik et al. 2019, Goudeau et al. 2021). We employed two strategies to express untagged TFAM at the *glh-1* locus: the viral 2A self-cleaving peptide system, which results in the production of two peptides via ribosomal skipping during translation (**Fig. 1A, left)**; and the *C. elegans SL2* trans-splicing recognition element (derived from the operonic gene *rla-1*), which causes the nascent transcript to be spliced into two independently translated mRNAs (**Fig. 1A, right)** (Nance and Frokjaer-Jensen 2019). We used CRIPSR/Cas9 genome engineering to insert either *T2A::TFAM* or *SL2::TFAM* at the 3' end of the endogenous *glh-1* protein coding sequence (**Fig. 1A**). To avoid known loss of functionality due to the presence of C-terminal tags on TFAM (Schwartz et al. 2022), we expressed TFAM untagged. Though we did not directly test for an increase of *TFAM* mRNA or TFAM protein, we presumed overexpression based on results below.

To determine the effect of overexpressing TFAM on mtDNA levels, we measured total mtDNA in whole L4 larvae by quantitative PCR (qPCR), as ~90% of total *C. elegans* mtDNA is derived from the germline (Tsang and Lemire 2002, Bratic et al. 2009). Both means of overexpressing TFAM resulted in a significant increase in mtDNA levels (~25-30%) (**Fig. 1B**). Conversely, as reported previously (Schwartz et al. 2022), we found that animals homozygous for a reduction-of-function *GFP*-tagged *TFAM/hmg-5* allele, here referred to as *TFAM-GFP (rf)*, had severe mtDNA copy number defects in L4 larvae (**Fig. 1B**). This defect in mtDNA number could be rescued by overexpressing TFAM in the *TFAM-GFP (rf)* background (**Fig. 1B**). Together, these results demonstrate that excess TFAM is sufficient to drive an increase in mtDNA levels in the *C. elegans* germ line.

We next sought to determine if increasing TFAM activity affected mtDNA quality. To accomplish this, we used a strain containing the *uaDf5* mtDNA deletion, which removes 3.1kb of the 13.8kb mitochondrial genome (Tsang and Lemire 2002). *uaDf5* deletes essential genes and therefore must exist in heteroplasmy with complementing wild-type mtDNA. Strikingly, *uaDf5* mutant mtDNAs persist stably over many generations due to the preferential replication of *uaDf5* mtDNAs over wild-type mtDNA genomes (Tsang and Lemire 2002, Gitschlag et al. 2020, Schwartz et al. 2022, Yang et al. 2022). Owing to this selfish replicative advantage, we hypothesized that excess TFAM would increase the proportion of *uaDf5* mtDNA relative to wild-type mtDNA. Indeed, *TFAM-O/E (T2A); uaDf5* adult animals contained a significantly higher percentage of mutant mtDNAs (~70%) compared to *uaDf5* controls (~60%) (**Fig. 1C**). This finding suggests that increasing mtDNA levels by overexpressing TFAM favors an even further expansion of *uaDf5* mutant genomes over wild-type mtDNAs compared to controls expressing normal TFAM levels.

Methods

Worm culture and strains

C. elegans strains were maintained at 20°C on nematode growth medium plates seeded with *Escherichia coli* OP50 as previously described (Brenner 1974). A list of all strains used/generated in the study is available in the *Strain Table* below.

Mitochondrial DNA quantification

For mtDNA copy number quantification, qPCR was performed exactly as previously described (Schwartz et al. 2022). Briefly, single late-L4 larvae were picked into 5µL of worm lysis buffer [50 mM KCl, 10 mM Tris-HCl (pH 8.0), 2.5 mM $MgCl_2$, 0.45% IGEPAL (Sigma I8896), and 200 µg/mL proteinase K (Invitrogen 2530049)] in PCR tubes, flash frozen at -80°C for 15 minutes, and lysed in a thermal cycler at 60°C for 1 hour followed by 15 minutes at 95°C. Larval worm lysates were diluted

with 95 µL of nuclease-free water (Invitrogen 4387936), and exactly 8µL of diluted lysate was used in triplicate for qPCR. Oligos targeting the mtDNA gene *nd-1* [*Fw: 5'- agcgtcatttattgggaagaagac -3' ; Rv: 5'- aagcttgtgctaatcccataaatgt -3']* were used. A standard curve using linearized plasmid containing the *nd-1* sequence was run for absolute quantification, and qPCR was performed using BioRad 2X SsoAdvanced Universal SYBR Green Supermix (BioRad 1725271) in a Roche LightCycler 480 machine as previously described (Schwartz et al. 2022).

For *uaDf5* heteroplasmy measurement, 60-100 whole adult animals were pooled in 60-100µL of worm lysis buffer in a screw cap 1.5mL microfuge tube, flash frozen at -80°C for 15 minutes, and lysed in a heating block at 60°C for 1 hour followed by 15 minutes at 95°C. Adult worm lysates were diluted 1000X and droplet digital PCR (ddPCR) quantification of *uaDf5* and WT mtDNA was performed exactly as previously described (Schwartz et al. 2022).

Plasmid construction

Plasmid pJN651 (*glh-1::SL2::YFP::PH::glh-1 3'UTR)* was constructed by replacing *GFP* in pDU92 (*glh-1::SL2::GFP::glh-1 3'UTR)* by Gibson assembly (Gibson et al. 2009).

CRISPR/Cas9 genome editing

CRISPR/Cas9-mediated genome editing was performed as described previously (Paix et al. 2017, Schwartz et al. 2022). Construction of *glh-1*(*xn127[glh-1::SL2::hmg-5])* required two steps. First, *glh-1(xn81[glh-1::SL2::yfp-PH]*) was generated using pJN651 as a PCR template to amplify *SL2::yfp-PH* with ~35 bps of homology for insertion at the C-terminus of endogenous *glh-1*. Second, for the generation of *glh-1*(*xn127[glh-1::SL2::hmg-5]),* N2 genomic DNA was used as a PCR template to amplify *hmg-5* with ~35bp of homology to replace *yfp-PH* by CRISPR at the *glh-1(xn81[glh-1::SL2::yfp-PH]*) locus. To generate *glh-1*(*xn167[glh-1::T2A::hmg-5])*, a single stranded oligonucleotide template was used to swap *SL2 for T2A* via CRISPR at the *glh-1*(*xn127[glh-1::SL2::hmg-5])* locus. Sequence files for all insertions are available upon request. All gRNA sequences are found in the ***Sequences Table*** below.

Statistical analysis and reproducibility

All statistical analysis was performed using GraphPad Prism 9 software. For all data, unpaired two-tailed Student's *t*-tests were performed, and where applicable no corrections for multiple comparisons were made to avoid type II errors (Armstrong 2014). Data in graphs are shown as Superplots (Lord et al. 2020). Three biologically independent experiments were performed for all experiments and the arithmetic means of biological replicates were used for statistical analysis.

Reagents

Strain Table:

Strain	Genotype	Source	Shorthand notation
FT2168	*naSi2 [mex-5p::mCherry-H2B::nos-2 3'UTR, unc-119(+)] II*	Nance Lab (*naSi2* transgene from (Roy, Kahler et al. 2018) outcrossed twice	WT in Fig. 1B
FT2278	*glh-1(xn167[glh-1::T2A::hmg-5]) I; naSi2 [mex-5p::mCherry-H2B::nos-2 3'UTR, unc-119(+)] II*	Nance Lab (This study)	*TFAM O/E (T2A)*
FT2217	*glh-1(xn127[glh-1::SL2::hmg-5]) I ; naSi2 [mex-5p::mCherry-H2B::nos-2 3'UTR, unc-119(+)] II*	Nance Lab (This study)	*TFAM O/E (SL2)*
FT2133	*xnSi45 [mex-5p::mCherry-MOMA-1::nos-2 3'UTR; unc-119(+)] II ; hmg-5(xn107[hmg-5-gfp]) IV*	Nance Lab (This study)	*TFAM-GFP (rf)*
FT2326	*glh-1(xn167[glh-1::T2A::hmg-5]) I; xnSi45 [mex-5p::mCherry-MOMA-1::nos-2 3'UTR; unc-119(+)] II ; hmg-5(xn107[hmg-5-gfp]) IV*	Nance Lab (This study)	*TFAM O/E (T2A); TFAM-GFP (rf)*

FT2285	*glh-1(xn127[glh-1::SL2::hmg-5]) I ; xnSi45 [mex-5p::mCherry-MOMA-1::nos-2 3'UTR; unc-119(+)] II; hmg-5(xn107[hmg-5-gfp]) IV*	Nance Lab (This study)	*TFAM O/E (SL2); TFAM-GFP (rf)*
FT2283	*glh-1(sam24[glh-1::gfp::3Xflag]) I ; xnIs510 [ehn-3::mCherry-PH, unc-119(+)] II ; uaDf5 / + mtDNA*	Nance Lab (This study)	*uaDf5* in Fig. 1C
FT2409	*glh-1(xn167[glh-1::T2A::hmg-5]) I ; xnIs510 [ehn-3::mCherry-PH, unc-119(+)] II; uaDf5 / + mtDNA*	Nance Lab (This study)	*TFAM O/E (T2A); uaDf5* in Fig. 1C
FT1917	*glh-1(xn81[glh-1::SL2::YFP-PH]) I; naSi2 [mex-5::mCherry-H2B::nos-2 3' UTR, unc-119(+)] II*	Nance Lab (This study)	See methods.

Sequences Table:

Name	**Sequence**	**Type/use**
glh-1 C-terminus gRNA	UCCCUCAAGAUGAAGAAGGC	Guide RNA to insert *SL2::yfp::PH* at the *glh-1* locus
ocrAS03	UACGAUUGAAGAAUGAGUAA	Guide RNA to replace *yfp::PH* with *hmg-5* in *xn81*
ocrAS04	ACUCCGGCUCCAUGGACCAG	Guide RNA to replace *yfp::PH* with *hmg-5* in *xn81*
ocrAS05	UUUAAUACAAGGUAACAACA	Guide RNA to replace *SL2* with *T2A* in *xn127*
ocrAS06	AACUUACGAUUGAAGAAUGU	Guide RNA to replace *SL2* with *T2A* in *xn127*

Acknowledgements: We would like to acknowledge Dustin Updike (MDI Biological Laboratory) for sharing reagents (plasmid pDU92) used in this study.

References

Armstrong RA. 2014. When to use the Bonferroni correction. Ophthalmic Physiol Opt 34: 502-8. PubMed ID: 24697967

Bratic I, Hench J, Henriksson J, Antebi A, Bürglin TR, Trifunovic A. 2009. Mitochondrial DNA level, but not active replicase, is essential for *Caenorhabditis elegans* development. Nucleic Acids Res 37: 1817-28. PubMed ID: 19181702

Brenner S. 1974. The genetics of *Caenorhabditis elegans*. Genetics 77: 71-94. PubMed ID: 4366476

Cagin U, Duncan OF, Gatt AP, Dionne MS, Sweeney ST, Bateman JM. 2015. Mitochondrial retrograde signaling regulates neuronal function. Proc Natl Acad Sci U S A 112: E6000-9. PubMed ID: 26489648

Ekstrand MI, Falkenberg M, Rantanen A, Park CB, Gaspari M, Hultenby K, et al., Larsson NG. 2004. Mitochondrial transcription factor A regulates mtDNA copy number in mammals. Hum Mol Genet 13: 935-44. PubMed ID: 15016765

Fu Y, Tigano M, Sfeir A. 2020. Safeguarding mitochondrial genomes in higher eukaryotes. Nat Struct Mol Biol 27: 687-695. PubMed ID: 32764737

Garrido N, Griparic L, Jokitalo E, Wartiovaara J, van der Bliek AM, Spelbrink JN. 2003. Composition and dynamics of human mitochondrial nucleoids. Mol Biol Cell 14: 1583-96. PubMed ID: 12686611

Gibson DG, Young L, Chuang RY, Venter JC, Hutchison CA 3rd, Smith HO. 2009. Enzymatic assembly of DNA molecules up to several hundred kilobases. Nat Methods 6: 343-5. PubMed ID: 19363495

Gitschlag BL, Tate AT, Patel MR. 2020. Nutrient status shapes selfish mitochondrial genome dynamics across different levels of selection. Elife 9:e56686. PubMed ID: 32959778

Goudeau J, Sharp CS, Paw J, Savy L, Leonetti MD, York AG, et al., Ingaramo M. 2021. Split-wrmScarlet and split-sfGFP: tools for faster, easier fluorescent labeling of endogenous proteins in *Caenorhabditis elegans*. Genetics 217: . PubMed ID: 33693628

Kanki T, Ohgaki K, Gaspari M, Gustafsson CM, Fukuoh A, Sasaki N, Hamasaki N, Kang D. 2004. Architectural role of mitochondrial transcription factor A in maintenance of human mitochondrial DNA. Mol Cell Biol 24: 9823-34. PubMed ID: 15509786

Larsson NG, Wang J, Wilhelmsson H, Oldfors A, Rustin P, Lewandoski M, Barsh GS, Clayton DA. 1998. Mitochondrial transcription factor A is necessary for mtDNA maintenance and embryogenesis in mice. Nat Genet 18: 231-6. PubMed ID: 9500544

Lewis SC, Uchiyama LF, Nunnari J. 2016. ER-mitochondria contacts couple mtDNA synthesis with mitochondrial division in human cells. Science 353: aaf5549. PubMed ID: 27418514

Lin YF, Schulz AM, Pellegrino MW, Lu Y, Shaham S, Haynes CM. 2016. Maintenance and propagation of a deleterious mitochondrial genome by the mitochondrial unfolded protein response. Nature 533: 416-9. PubMed ID: 27135930

Lord SJ, Velle KB, Mullins RD, Fritz-Laylin LK. 2020. SuperPlots: Communicating reproducibility and variability in cell biology. J Cell Biol 219:e202001064. PubMed ID: 32346721

Maniura-Weber K, Goffart S, Garstka HL, Montoya J, Wiesner RJ. 2004. Transient overexpression of mitochondrial transcription factor A (TFAM) is sufficient to stimulate mitochondrial DNA transcription, but not sufficient to increase mtDNA copy number in cultured cells. Nucleic Acids Res 32: 6015-27. PubMed ID: 15547250

Marnik EA, Fuqua JH, Sharp CS, Rochester JD, Xu EL, Holbrook SE, Updike DL. 2019. Germline Maintenance Through the Multifaceted Activities of GLH/Vasa in *Caenorhabditis elegans* P Granules. Genetics 213: 923-939. PubMed ID: 31506335

Matsuda T, Kanki T, Tanimura T, Kang D, Matsuura ET. 2013. Effects of overexpression of mitochondrial transcription factor A on lifespan and oxidative stress response in *Drosophila melanogaster*. Biochem Biophys Res Commun 430: 717-21. PubMed ID: 23206694

Matsushima Y, Garesse R, Kaguni LS. 2004. *Drosophila* mitochondrial transcription factor B2 regulates mitochondrial DNA copy number and transcription in schneider cells. J Biol Chem 279: 26900-5. PubMed ID: 15060065

Nance J, Frøkjær-Jensen C. 2019. The *Caenorhabditis elegans* Transgenic Toolbox. Genetics 212: 959-990. PubMed ID: 31405997

Otten ABC, Kamps R, Lindsey P, Gerards M, Pendeville-Samain H, Muller M, van Tienen FHJ, Smeets HJM. 2020. *Tfam* Knockdown Results in Reduction of mtDNA Copy Number, OXPHOS Deficiency and Abnormalities in Zebrafish Embryos. Front Cell Dev Biol 8: 381. PubMed ID: 32596237

Paix A, Folkmann A, Seydoux G. 2017. Precision genome editing using CRISPR-Cas9 and linear repair templates in *C. elegans*. Methods 121-122: 86-93. PubMed ID: 28392263

Roy D, Kahler DJ, Yun C, Hubbard EJA. 2018. Functional Interactions Between *rsks-1/*S6K, *glp-1/*Notch, and Regulators of *Caenorhabditis elegans* Fertility and Germline Stem Cell Maintenance. G3 (Bethesda) 8: 3293-3309. PubMed ID: 30126834

Schwartz AZA, Tsyba N, Abdu Y, Patel MR, Nance J. 2022. Independent regulation of mitochondrial DNA quantity and quality in *Caenorhabditis elegans* primordial germ cells. Elife 11:e80396. PubMed ID: 36200990

Sumitani M, Kasashima K, Matsugi J, Endo H. 2011. Biochemical properties of *Caenorhabditis elegans* HMG-5, a regulator of mitochondrial DNA. J Biochem 149: 581-9. PubMed ID: 21258070

Tsang WY, Lemire BD. 2002. Mitochondrial genome content is regulated during nematode development. Biochem Biophys Res Commun 291: 8-16. PubMed ID: 11829454

Tsang WY, Lemire BD. 2002. Stable heteroplasmy but differential inheritance of a large mitochondrial DNA deletion in nematodes. Biochem Cell Biol 80: 645-54. PubMed ID: 12440704

Wang LJ, Hsu T, Lin HL, Fu CY. 2021. Modulation of mitochondrial nucleoid structure during aging and by mtDNA content in *Drosophila*. Biol Open 10:bio058553. PubMed ID: 34180963

2/14/2023 - *Open Access*

Yang Q, Liu P, Anderson NS, Shpilka T, Du Y, Naresh NU, et al., Haynes CM. 2022. LONP-1 and ATFS-1 sustain deleterious heteroplasmy by promoting mtDNA replication in dysfunctional mitochondria. Nat Cell Biol 24: 181-193. PubMed ID: 35165413

Funding: New York State Stem Cell Science (C32560GG) - AZAS ; Eunice Kennedy Shriver National Institute of Child Health and Human Development (F31HD102161) - AZAS ; National Institute of General Medical Sciences (R35GM118081) - JN

Author Contributions: Aaron Z.A. Schwartz: writing - original draft, conceptualization, formal analysis, investigation. Jeremy Nance: writing - original draft, supervision, resources.

Reviewed By: Anonymous

History: Received December 20, 2022 **Revision Received** February 9, 2023 **Accepted** February 13, 2023 **Published Online** February 14, 2023 **Indexed** February 28, 2023

Citation: Schwartz, AZA; Nance, J (2023). Germline TFAM levels regulate mitochondrial DNA copy number and mutant heteroplasmy in *C. elegans*. microPublication Biology. 10.17912/micropub.biology.000727